Batteries & Supercaps

Minireviews
doi.org/10.1002/batt.202000332

Chemistry Europe
European Chemical Societies Publishing

VIP *Very Important Paper*

Special Collection

Recent Advances in Alkali Metal-Ion Hybrid Supercapacitors

Lishuang Xia,[a] Bin Tang,[a] Jinping Wei,*[a] and Zhen Zhou*[b]

An alkali metal-ion hybrid supercapacitor is composed of a battery-type electrode and a capacitor-type one, with alkali metal ions transporting in the bulk of the whole device. In brief, batteries and supercapacitors are systematically combined in alkali metal-ion hybrid supercapacitors accompanying with the fusion of both merits and exceptional performances. Such hybrid devices can deliver both high energy and power density, as well as long cycle life. In this review, the energy storage mechanisms, electrode materials and electrolytes are summarized for alkali metal-ion hybrid supercapacitors, focusing on recent advances, current problems and future perspectives.

1. Introduction

Traditional fossil fuels are not renewable and the contamination produced from fuels has troubled people for long. New energy sources such as solar, wind, and wave energy are investigated but they are still restricted from discontinuity and instability which make them hard for sequentially stable energy supply. Electrochemical energy storage (EES) devices are devised to make difference. Among them, lithium ion batteries (LIBs) and supercapacitors (SCs) are successful and firstly commercialized. LIBs possess high energy density (150 ~ 200 Wh kg^{-1}) but relative low power density (< 1 kW kg^{-1}).[1,2] During (dis)charging process, the electrode materials go through repeated expansion and shrinkage, resulting in the structure change, which causes the instability of the whole cell. Moreover, the overcharge and lithium dendrites still threat to battery safety. SCs based on ion adsorption on surface contributing to quick (dis)charging deliver high power density, but still suffer from low energy density (20 ~ 30 Wh kg^{-1}). Since no chemical reaction undergoes within electrode materials, supercapacitors are stable and safe.[3] To meet the demand of modern society, batteries and supercapacitors are coupled creatively to get unique devices with enhanced characteristics.[4] A new-type device is emerging with high energy density and impressive power density, which is named as metal-ion hybrid supercapacitors (MHSs). Alkali metal-ion hybrid supercapacitors (AMHSs)[5] consist of lithium ion hybrid supercapacitors (LIHSs),[6] sodium ion hybrid supercapacitors (SIHSs),[7] and potassium ion hybrid supercapacitors (KIHSs).[8]

Up to now, LIBs are the most successful rechargeable batteries, and their electrodes are firstly applied to MHSs as battery-type electrodes, which can be classified as LIHSs.[9] However, due to the limited abundance of lithium resources, sodium and potassium are expected to be ideal alternatives for their relative large reserves. The proportion of Na in the crust is 2.36 wt%, comparable to 2.09 wt% of K (Li, 0.002 wt%).[10,11] Meanwhile, Na exhibits similar negative redox potential of −2.71 V *vs.* SHE (Standard hydrogen electrode) in aqueous media, and K shows lower electrode potential of −2.93 V (Li, −3.04 V). Both Na and K show almost the same large-scale storage capability and low cost, but the unique merit of sodium vs. potassium is that Na ions have smaller ionic radius of 1.02 Å, compared with 1.38 Å of K ions (Li^+, 0.76 Å). These two elements possess weaker Lewis acidity and relative lower redox potential. Besides, K^+ can utilize graphite as electrodes. These unique merits endow sodium/potassium with irreplaceable positions.

In this review, the latest advances on both electrodes and electrolytes of AMHSs are summarized. Firstly, three typical storage mechanisms are analyzed. Then, based on energy storage mechanisms, two different kinds of electrodes are classified as battery-type and capacitor-type ones. The main factors influencing electrochemical performances are discussed. Also, researchers provide various modification and improvement strategies for these obstacles including carbon coating, heteroatom doping, nanostructural construction, *etc.* for electrodes, which are summarized in detail on basis of the kinds of materials. Besides, except for aqueous and organic electrolytes, ionic liquids and quasi-solid-state electrolytes, which effectively satisfies the demand from the development of MHSs, are also introduced. Finally, new insights are put forward for the future applications and opportunities.

[a] *L. Xia, B. Tang, Prof. J. Wei*
School of Materials Science and Engineering
Institute of New Energy Material Chemistry
Renewable Energy Conversion and Storage Center (ReCast)
Key Laboratory of Advanced Energy Materials Chemistry (Ministry of Education)
Nankai University
Tianjin 300350, P. R. China
E-mail: jpwei@nankai.edu.cn

[b] *Prof. Z. Zhou*
Engineering Research Center of Advanced Functional Material Manufacturing of Ministry of Education
School of Chemical Engineering
Zhengzhou University
Zhengzhou 450001, P. R. China
E-mail: zhenzhou@zzu.edu.cn

Special Collection *An invited contribution to a Special Collection dedicated to Metal-Ion Hybrid Supercapacitors*

2. Alkali Metal-Ion Hybrid Supercapacitors

Batteries and capacitors are both invented for electrochemical energy storage. In order to achieve better performance and satisfy the booming need for large-scale electric application, AMHSs are put forward. Compared with other energy storage devices, AMHSs show many unique preponderances. The advantages from both LIBs and SCs are integrated such as high energy density, high power density and long cycling lifespan. As expected, the defects are also "boarding this ship" and researchers are trying their best to avoid these annoying flaws.

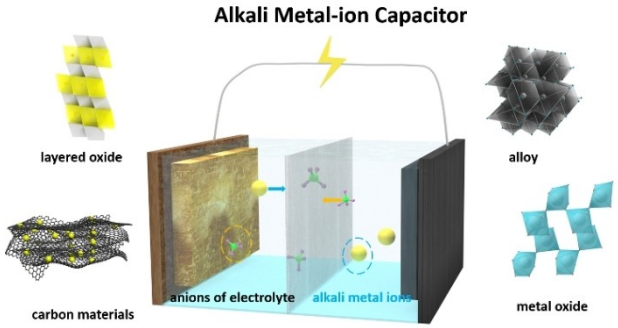

Figure 1. Schematic illustration of MHSs based on an electrolyte consuming mechanism

2.1. Mechanisms of Alkali Metal-Ion Hybrid Supercapacitors

In general, AMHSs consist of two kinds of electrodes which are battery-type and capacitor-type ones, and the energy storage mechanism of MHSs should be considered from both electrodes (Figure 1). The anions from electrolytes are adsorbed on the interface between the cathode and electrolyte. This is a fast physical procedure with high power density. The alkali metal ions also play an important role in providing the most part of energy density. Alkali metal ions exhibit (de)intercalation process during energy storage, and sometimes there also exits adsorption/desorption on the surface.

Metal-ion hybrid supercapacitors consist of electrodes based on Nernstian storage as well as capacitive electrodes. So, the storage mechanisms of MHSs include two parts: redox reactions based on metal ion (de)intercalation, and reversible adsorption of ions on the surface. Compared with metal-ion batteries, MHSs possess higher power density but lower capacity due to the limited chemical redox reactions provided from battery-type electrodes. Compared with traditional supercapacitors, it shows higher energy density but lower power output owing to physical adsorption stemmed from capacitor-type electrodes. It is significant to couple compatible electrodes to achieve the combination of advantages with relatively less defect.

There are three energy storage mechanisms as follows.

2.1.1. Electric Double-Layer Capacitance

The mechanism of capacitor-type electrodes is based on electric double-layer capacitance (EDLC), which is capacitance-type energy storage from electric double layer (EDL), namely, the interface between the electrode and electrolyte provides electrochemical polarization, and then EDL occurs in the interface to store charge. During charging, electrodes can realize the reversible adsorption of opposite-charge ions from the electrolyte, and the charge retains in EDL. In this process,

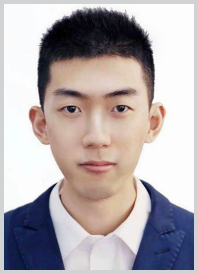

Lishuang Xia was born in Shandong, China. He obtained his bachelor's degree in materials chemistry at Beijing Jiaotong University in 2018. Now he is pursuing his master degree at Nankai University in Prof. Zhen Zhou's group, majoring in materials physics and chemistry. His research interest mainly focuses on materials design for lithium and sodium ion batteries.

Bin Tang was born in Shandong, China. He received B.S. degree in School of Chemistry and Chemical Engineering from Ocean University of China in 2016. Now he is working toward a Ph.D. degree in School of Materials Science and Engineering, Nankai University, supervised by Prof. Zhen Zhou. His research focuses on solid-state electrolytes for lithium-ion and sodium-ion batteries.

Jinping Wei was born in Jiangxi, China. He received B.S. in 1987, majoring in chemistry from Xiamen University, China. After three years of educational work, he came to Nankai University for further study and received his M.S. in 1993 and PhD in 2003. In 2005, he worked in Monash University, Australia as a visiting scholar. Since 1993, he has been working in Nankai University. His research interest focuses on materials for lithium and sodium ion batteries.

Zhen Zhou received his BSc (applied chemistry, in 1994) and PhD (inorganic chemistry, in 1999) from Nankai University, China. He joined the faculty at Nankai University as a lecturer in 1999. Two years later, he began to work as a postdoctoral fellow in Nagoya University, Japan. In 2005, he returned to Nankai University as an associate professor and was promoted as a full professor in 2010. In 2020, he was admitted as a Fellow of RSC (FRSC). In 2021, he moved to Zhengzhou University, China as a distinguished professor. His main research interest is new energy science and engineering.

there is no chemical reaction and this physical process is reversible. The concept of EDL was first proposed by von Helmholtz[12] and revised by Gouy[13] and Chapman,[14] and then improved by Stern.[15] The final revised calculation formula for EDL capacitance is $1/CDL = 1/CH + 1/CD$. Due to the high concentration of electrolytes, the diffusion layer is so thin that the CD could be ignored, resulting in $CDL \approx CH$. Here CDL, CH and CD are the capacities of double electric layer (in Stern model), compact double electric layer (in Helmholtz model), and diffuse layer (in Gouy and Chapman (GC) model), respectively.

2.1.2. Nernstian Storage

The mechanisms of battery-type electrodes are classified as Nernstian storage and pseudocapacitance.

Nernstian storage follows the Nernst equation, which is a battery-like behavior. The active materials are traditional electrode materials for batteries. The storage mechanism of battery-type electrodes is based on the transportation of metal ions (Li^+, Na^+, *etc.*) between two electrodes, at the mean time a reversible (de)intercalation or redox reaction. Usually this kind of materials possess high capacity. But due to the limitation of metal-ion diffusion kinetics, the (de)intercalation is much sluggish compared with adsorption, resulting in lower rate capability.

2.1.3. Pseudocapacitance

Pseudocapacitance is a special energy storage behavior that seems to be capacitive.[16] However, it stems from electrochemical processes and relates to charge transfer reactions (Figure 2). The energy storage mechanism of pseudocapacitance is that active substances proceed underpotential deposition on the electrode surface or bulk, and the highly reversible redox reaction produces the capacitance associated with the potential. *Pseudocapacity* was first used to describe an electrochemical redox process related with near surface adsorption by Grahame.[17] Conway[18] proposed that due to the Faraday process on the surface of electrode materials, which is different from EDLC based on ion adsorption, pseudocapacitance is not the traditional capacitance. But this surface-charge transfer reaction associated with underpotential deposition is very limited and shows a narrow voltage range resulting in low overall charge. Up to now, pseudocapacitance mechanisms can be divided into two types: surface redox and intercalation pseudocapacitance. For example, some metal oxides are typical surface redox pseudocapacitance materials, such as ruthenium oxide and manganese dioxide in aqueous electrolytes. A type of 2D materials named MXene has been applied in EES systems with eminent pseudocapacitive performance. Moreover, some metal oxides like TiO_2 and *T*-Nb_2O_5 display a Li^+ intercalation pseudocapacitance. Involving the chemical reaction, pseudocapacitance has about 1000 times higher capacity than that of EDLC and it is comparable to some batteries. Moreover, it can realize quick (dis)charge which is almost on par with EDLCs in some cases. This special property makes pseudocapacitance-type materials very promising for large-scale energy storage, and can satisfy the needs for large energy density with fast storage from social development.

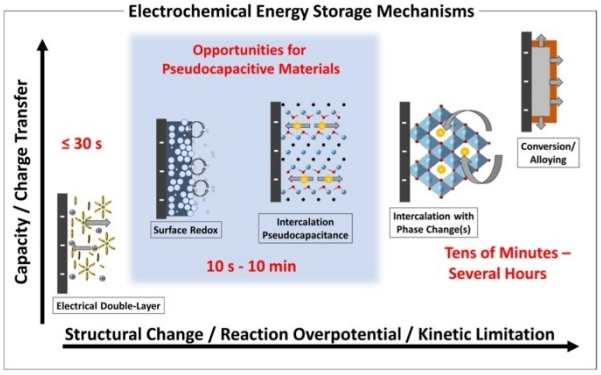

Figure 2. Classification of electrochemical energy storage mechanisms as a function of their characteristic capacity and the associated degree of structural changes of the electrodes, reaction overpotential, and kinetic limitations. Pseudocapacitive materials should provide short cycling times of about 10 s to 10 min while exhibiting capacities associated with intercalation mechanisms. Reproduced from Ref. [16] with permission. Copyright (2020) American Chemical Society.

2.2. Bottlenecks Encountered

LIHSs, as the most studied hybrid supercapacitors, have already been applied as commercial EES devices since 2005. The energy density of LIHSs is almost achieved at the same magnitude level of LIBs, although there is still room for improvement of power energy compared with supercapacitors. Then more and more metal elements are investigated as substitutes for lithium due to their unique merits. So, when the concept of AMHSs came into being, it attracted much attention rapidly, and have grown to blossom in recent years.

However, challenges are still in the front of researchers, and vast efforts are needed.

Limited power proficiency has been the problem in the breach since MHSs were proposed. This problem has been bothering scientists for a long time and until now the perfect solution has not been found. Although battery-type electrodes possess high specific energy, they usually do not match perfectly with fast-kinetics capacitive electrodes, which indicates that the power density of electrochemical intercalation electrodes have to be promoted urgently. Due to the fast adsorption and desorption of ions from capacitor-type electrodes, the diffusion and transportation of metal ions in battery-type electrodes are the main factors that limited the power density, especially the sluggish kinetics of metal ions in the bulk of materials.[19] Fortunately some strategies were proposed to push AMHSs up to their best.

Moreover, the insufficient energy density compared with metal-ion batteries is another reason hindering the further application of MHSs. Obviously, capacitor-type electrodes

determine the capacity of the whole device. Similarly, the imperfect compatibility also affects the energy density of the whole device. Low capacitance is the inevitable side effect brought by fast-kinetics behavior from capacitor-type electrodes. Nanoscale and porous structures are effective ways to provide lager surface area and more active sites to endow more capacitance.

The intrinsic nature of AMHSs restricts their upper limit. The common AMHSs are composed of traditional battery-type electrodes and capacitor-type electrodes, which suggests that they cannot break the ceilings of traditional batteries and capacitors. Meanwhile, it is hard to choose perfectly-matched pairs of different electrodes. It inspires people to find a different way to assemble brand new systems of hybrid devices.

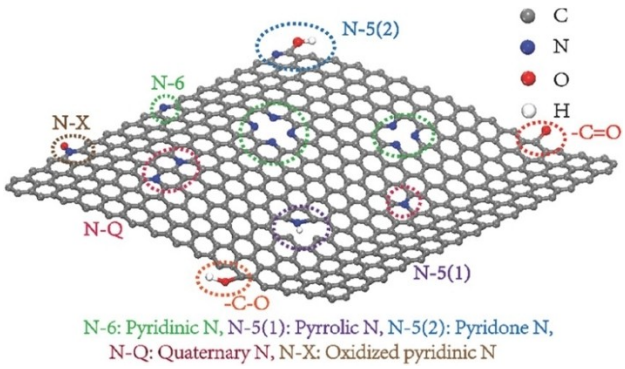

Figure 3. Various N-containing functional groups in graphene. N-6: Pyridinic N; N-5(1): Pyrrolic N; N-5(2): Pyridone N; N–Q: Quaternary N; N–X: Oxidized pyridinic N. Reproduced from Ref. [20] with permission. Copyright (2017) The Author(s).

2.3. Strategies Proposed

Many strategies were proposed to push AMHSs up to their best. People pin their hope on AMHSs to make breakthrough in EES devices. Solutions are various from materials to materials but they can be classified as, novel materials for both electrodes and electrolytes, novel architectures such as nanostructures and porous structures, surface modifications with functional materials such as conductive coating, volume buffers, and heteroatom doping to facilitate electron transportation or to stabilize the framework, and formation of composites such as carbon materials with metal oxides.

AMHSs suffer from the rapid capacity decay during cycling, which significantly restricts its further application and development. This problem mainly results from the incompatibility between electrodes and electrolytes as well as the structure instability of battery-type electrodes during the (de) intercalation of metal ions. It is important to choose appropriate anodes and cathodes.

As for battery-type electrodes, the main methods include carbon coating for metal-salt-type materials and heteroatom doping for carbonaceous materials to get better kinetics and shorter diffusion length. Carbon matrixes for other active materials can provide higher electronic conductivity, which facilitates charge transportation, provides large contact area with electrolytes, and stabilizes structures to accommodate the volume change during fast (dis)charging. Heteroatom doping (such as nitrogen doping in graphene, Figure 3)[20] can provide increased electrical conductivity as more electrons are brought to the delocalized π-system of carbon materials, and enhanced capacity owing to additional redox reactions for pseudocapacitance.[21]

To achieve excellent electrochemical performance, large surface area and suitable pore distribution are the main factors for capacitor-type electrodes. As mentioned above, more pores might not bring better performance, and suitable pore size distribution is needed. As for battery-type electrode materials, carbon coating, heteroatom doping and nanostructures are beneficial. Some materials like $LiCoO_2$[22] and $Li_4Ti_5O_{12}$[23] might show capacitor-like behavior rather than battery-like one when they are in ultra-small nanosizes (diameters <10 nm). After further investigations, scientists believed that it is the enhanced exterior surface area that causes this unique phenomenon.

Moreover, to get decent electrochemical performance in MHSs, electronic conductivity should be taken into consideration. The whole device is restricted and influenced by internal resistance, which is composed of the contact resistance between electrodes and electrolytes, the inner resistance in electrodes introduced by binders, etc., and the diffusion resistances of ions in electrodes. High surface area and porosity are needed for both electrodes and electrolytes, but the pore size distribution should be carefully chosen. Different kinds of electrolytes possess various properties which are suitable for different sizes of metal ions and kinds of electrodes.

2.4. Main Features

As mentioned above, AMSHs, with alkali ions as charge carriers, possess these characteristics:

(a) two kinds of electrodes, one battery type and one capacitor type.
(b) high energy (to the battery level) and power (to the supercapacitor level) density.
(c) "AMSH-type" charge-discharge and cyclic voltammetric (CV) curves.
(d) function in a wide voltage window or at a high voltage.

Several conventional electrodes in ion batteries are directly used in AMSHs such as $LiFePO_4$ and $LiCoO_2$. However, their sluggish diffusion kinetics makes them unapt choice to match with the high power capacitor-type cathode. So, these materials need to be modified until the high energy (to the battery level) and power (to the supercapacitor level) density will be achieved in the devices. Then, the intrinsic factor to define AMSHs is the electrochemical characteristics, which means that charge-discharge and CV curves are "AMSHs-type". The typical charge-discharge curves (Figure 4a) and CV curves (Figure 4b) of supercapacitors are bending without any redox peak or plateau which exists in batteries (Figure 4e and f). For pseudocapacitors, they are compromise curves (Figure 4c and d) between supercapacitors and batteries. Hence, the charge-

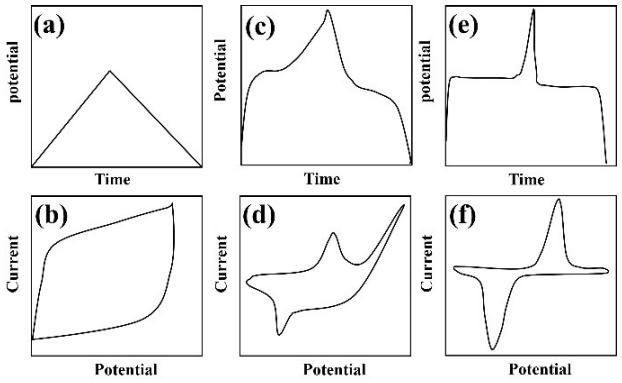

Figure 4. Charge-discharge and CV curves for supercapacitors (a,b), pseudocapacitors (c,d), and LIBs (e,f).

discharge curves for AMSHs should be linear without distinct plateaus and the CV curves should be nearly straight without any obvious peak. Moreover, it is necessary for the hybrid device to operate in a wide voltage window. The capacitor-type cathode without involving electrode reactions between lithium ions and active materials could work at a high potential and the potential as low as that of alkali metals of battery-type anodes can be achieved by prelithiation/presodiation. Thus, it is possible to get a wide voltage window.

In this review, devices without satisfying these features mentioned above, are not regarded as AMHSs.

3. Three Systems for AMHSs

According to the above discussion on mechanisms, AMHSs are classified into three systems as 'Nernstian storage//EDLC', 'pseudocapacitance//EDLC', and 'Nernstian storage//pseudocapacitance'. Note that the anode and cathode are relative, determined on which one possesses lower or higher potential. For example, some capacitor-type electrodes such as the commercial activated carbon (AC) can be the anode or cathode according to different conditions. There are some general requirements for getting well-matched and highly compatible AMHSs.

Requirements for battery-type electrodes: (a) The mechanisms should be Nernstian storage or pseudocapacitance. Generally, they provide much larger capacity than capacitor-type materials. In this case, the energy density of AMHSs is mainly restricted by capacitor-type electrodes. (b) The kinetics of metal ions in materials should be outstanding. It requires higher ion diffusion and faster electron transport in order to achieve better match with capacitor-type electrodes. (c) The stability of battery-type materials should be aware due to the severe decay during ion de/intercalation. It needs much higher stability for battery-type electrodes, and the modifications for them are basically focused on this aspect.

Requirements for capacitor-type electrodes: (a) The mechanism should be EDLC, noting that the pseudocapacitor materials under some circumstances can satisfy the requirements for capacitor-type electrodes. Generally, they provide higher stability and faster kinetics than battery-type electrodes. In this case, the power density of AMHSs is mainly restricted by battery-type electrodes. (b) The capacity of capacitor-type materials should be large. Due to EDLC, they exhibit much less capacity which is the main factor that hinders the energy density of the whole device. To match high-capacity battery-type electrodes, high-capacity capacitor-type materials are necessary.

3.1. Nernstian Storage//EDLC

3.1.1. Metal Polyoxometalates//AC

Typical battery-type cathode materials for AMHSs are silicates or phosphates ($LiFePO_4$ (LFP),[28,29] $Li_3V_2(PO_4)_3$ (LVP),[30,31] $LiMnPO_4$ (LMP),[32] *etc.*). Those materials possess high theoretical capacity (170 $mAh\,g^{-1}$ for LFP), low cost and outstanding thermal durability, but the limited Li^+ diffusion kinetics and poor electronic conductivity make the performance less than satisfactory. They can be electrodes with further improvement.

Recently, some strategies have been proposed to refine its defects, and the common way is assembling it with carbon materials to fabricate bifunctional composites. Zhang *et al.*[24] reported LFP particles embedded in reduced graphene oxide (rGO) coated LVP@C nanosheets as LIHS cathodes (Figure 5). The rate performance is attractive that at 15 $A\,g^{-1}$ (100 C) ultrahigh current density, the capacity can maintain 71 $mAh\,g^{-1}$. Moreover, it showed a long lifespan at 10 $A\,g^{-1}$ (67 C), and the capacity retention is still about 70%. Via ab initio molecular dynamic simulations, Li^+ diffusion coefficient of LFP was thousand times lower than that of LVP, indicating that LVP was the main contributor to rate performance. Meanwhile, the electrons tended to transport from Li atoms to pyridinic-N or pyrrolic-N doping, which strengthened the interaction between LFP and graphene as well as the electronic conduction. When the above cathodes were matched with commercial AC anodes, the devices delivered an energy density

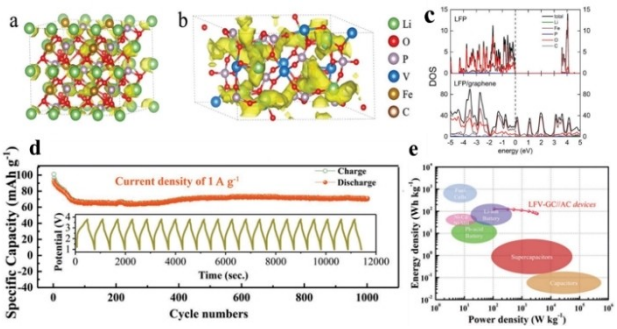

Figure 5. Li^+ probability density distribution in a) LFP and b) LVP obtained from 10 ps AIMD simulations at 1000 K, the isosurface (yellow) of Li^+ probability density is plotted at isovalue of $0.001/a_0^3$ (a_0 is the Bohr radius); c) PDOS of LFP and LFP/graphene interface; the Fermi level is set to 0 eV and plotted as a dashed line; d) Cycling performance at 1 $A\,g^{-1}$ of LFV-GC//AC full cells; e) Ragone plot of LFV-GC//AC full cells and device-based performance for the currently available energy-storage systems. Reproduced from Ref. [24] with permission. Copyright (2019) Wiley-VCH.

of 77 Wh kg^{-1} at power density of 108.6 W kg^{-1} at 0.1 A g^{-1}. Even at 5 A g^{-1} with the power density up to 3.36 kW kg^{-1}, the energy density could also sustain 77 Wh kg^{-1}. The result showed great potential of this material for LIHSs.

Moreover, heteroatom doping[25] is also an effective approach. Secchiarol *et al.*[25] synthesized $Li_3V_{2-x}Ni_x(PO_4)_3$/C (x = 0, 0.05, and 0.1) as LIHS cathodes. In the voltage window of 3.0–4.0 V, the specific discharge capacity is 93 mA h^{-1} at 100 C and the retention of capacity is 97% even after 1000 cycles. With a commercial AC anode, the device delivered a high energy density of 18.7 Wh L^{-1} at a power density of 2.58 kW L^{-1}.

3.1.2. Metal Oxides//AC

Metal oxides [34–37] are common cathode materials for ion batteries; when applied for AMHSs, they need large modification. There is a special kind of oxides named layered transition metal oxides, and classified as P2- and O3-Type materials in which alkali metal ions occupy octahedral and prismatic sites, respectively. These oxides usually suffer from structure change and low capacity and heteroatom (Ni,[33] Co,[26] Mn,[27] etc.) doping is an efficient method to deal with these defects.

3.1.3. Metalloid Materials//AC

Carbon materials (graphite, hard carbon (HC), and soft carbon) are widely used as electrodes due to low cost and environmental friendliness.

When graphite is utilized as the anode for AMHSs, it is usually doped with heteroatoms.[44–64] For example, pre-lithiated graphite was fabricated as anodes by Sivakkumar *et al.*,[38] which was assembled with AC cathodes. The LIHSs delivered energy density of 55 Wh kg over the potential range of 3.1–4.1 V. Two kinds of hard carbon (spherical HC and irregular HC)[39] were pre-lithiated and assembled with AC cathodes to fabricate LIHSs.

HC demonstrated a good anode material for SIHSs. Graphite, which is widely used in LIHSs, is thermodynamically not suitable for sodium ion batteries. Because compared with Li^+ (6.94, 0.76 Å), Na^+ has lager atomic mass (22.99) and ionic radius (1.02 Å) with the additionally sluggish kinetics, it is hard for Na^+ to intercalate into graphite. Usually, hard carbon would be handled with presodiation firstly. Kuratani *et al.*[40] utilized presodiated hard carbon as anodes for SIHSs with AC cathodes. The devices delivered long cycling life of retaining more than 90% capacity over 1000 cycles. At a high current rate of 45 C, they showed equally matched capacity retention (70%) compared with LIHSs. The presodiation significantly influences the electrochemical performance.

While enlarging the interlayer space, carbon materials showed competitive rate capability and cycling span. Recently, Chen *et al.*[41] have reported disordered carbon nanosheets with large interlayer space as anodes for KIHSs. This oxygen-rich material possessed good stability (80% capacity retention after 5000 cycles) and outstanding rate capability. Combined with the AC cathode, this device delivered high energy density of 149 Wh kg^{-1} as well as power density of 21 kW kg^{-1} at voltage up to 4.2 V. Moreover, introducing heteroatoms to carbon materials can dramatically promote the rate capability.

Si possesses good merits such as high theoretical specific capacity (4200 mAh^{-1} as crystalline Si)[54] and low Li insertion/extraction potential. But severe volume expansion results in poor stability and limits its application. Si was firstly introduced into hybrid capacitors by Konno *et al.*[42] in the glass-like form of SI–C-O as anodes. Recently it has been improved by incorporating with carbon. Li *et al.*[43] prepared porous Si@C ball-in-ball hollow spheres as battery-like anodes for lithium-ion capacitors. Unlike traditional Si/C core-shell structures, the new yolk-shell structure is able to provide sufficient void space for buffering the huge volume changes of Si. The capacitors based on porous Si@C hollow spheres showed high energy densities of 239 and 154 W h kg^{-1} at power densities of 1376 and 69600 W kg^{-1}, respectively, and the cycling performance was improved with stable 15000 cycles at 6.4 A g^{-1}.

3.1.4. Metal Chalcogenides//AC

Metal chalcogenides possess large interlayer space and high specific capacity, but suffer from poor structural stability and severe capacity decay during metal ion insertion/extraction processes. Many strategies have been proposed to improve the performance such as modification of interlayer spaces, nanocrystallization and coating with carbon materials.

Metal sulfides such as MoS_2 are representative 2D layered materials, which possess many disadvantages such as the instable structure during the (de)intercalation of Li^+. The most effective way is coating with carbon. In recent years, efforts have been made to modify the interlayer space of MoS_2, and achieve nanoscale structures. By incorporating RGO, MoS_2 was demonstrated to reveal pseudocapacitive characteristics and increased atomic interface contact.[84]

Metal selenides suffer from similar problems to sulfides owing to the alike properties of S and Se as chalcogenides.[84–87] Volume changes during charging-discharging processes restrict the cycling stability which can also be alleviated by incorporating with carbon materials.

3.1.5. Metal Nitrides and Phosphides//AC

Metal nitrides are pseudocapacitance-type materials such as NbN which can be prepared by nitridation of Nb_2O_5. Wang *et al.*[88] have recently prepared p-NbN by the direct nitridation of the Nb_2O_5 commercial powder, and the porous property was kept during this process which contributed to the conductivity. When combined with AC to fabricate LIHSs, and cycled within a voltage window between 0 to 4.0 V, they delivered a high energy density of 149 Wh kg^{-1} and power density of 45 kW kg^{-1}. The capacity retention was 95% after 15000 cycles at 1.0 A g^{-1}. After combined with nitrogen-doped graphene nanosheets by Liu *et al.*,[89] this hybrid material delivered high

energy density of 122.7–98.4 W h kg^{-1} at power density of 100–2000 W kg^{-1}.

Transition metal phosphides are considered as promising materials for electrochemical energy storage due to their high theoretical capacity. But they also suffer from severe capacity fading resulting from large volume expansion. RGO is often utilized to accommodate and alleviate the volume change.

3.1.6. Metal Polyoxometalates//AC

The spinel-structured $Li_4Ti_5O_{12}$ (LTO) is also an attractive anode material due to its high capacity and structural stability. But the low conductivity restricts its performance. Assembling with graphene would alleviate this problem. Wang *et al.*[90] fabricated a composite of nanosized $Li_4Ti_5O_{12}$ (LTO) and graphene nanosheets via an atomic layer deposition (ALD) seeded process incorporated with hydrothermal lithiation (Figure 6). The composite delivered a high reversible capacity of 120.8 mAh g^{-1} even at 100 C. LIHSs can be charged/discharged to about 70% of the theoretical capacity of LTO in 25 s and even after 2500 cycles at 20 C, and the capacity retention was still 90%. Similarly, $Zn_2Ti_3O_8$,[91] $TiNb_2O_7$,[92] *etc.* have also been investigated.

$Na_2Ti_3O_7$[96] and $K_2Ti_6O_{13}$[95] proved to have sodium and potassium storage ability, and at low voltage it is possible for sodium ions to show intercalation/deintercalation behavior. Meanwhile, the merits of low cost and amply resources attract much attention. They are relatively stable and less volume change occurs during charging/discharging processes, but the low electronic conductivity of metal salts has still been bothering researchers for years. Many strategies were proposed to promote the performance, such as building nanostructures[93] and coating with carbon materials.[94]

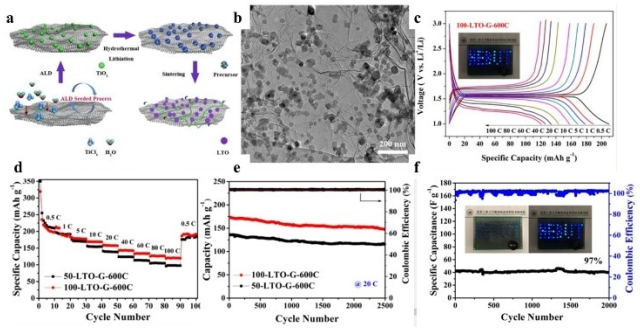

Figure 6. a) Schematic illustration of a typical ALD seeded process incorporated with hydrothermal lithiation and the as-obtained LTO/graphene composites; b) TEM image; c) Charge/discharge potential profiles; d) Cycling rate performance and e) cyclic stability of the LTO/graphene composites; f) Cyclic performance of a LIHS full cell and (inset) digital images of one LIHS full cell before and after lighting up 48 blue LEDs. Reproduced from Ref. [90] with permission. Copyright (2017) Elsevier.

3.1.7. Other Materials//AC

Some metals can alloy with alkali metals such as Sn,[102] and provide huge capacity but dramatic volume change. Lang *et al.*[103] reported a flexible Sn//AC KIHS, which delivered a high energy density of 120 W h kg^{-1} and power density of 2850 W kg^{-1}. It showed good cycling stability with the capacity maintaining about 75 mAh g^{-1} over 2000 cycles at 3.0 A g^{-1} and excellent rate performance. These results suggest the potential for high-performance EES applications.

3.2. Pseudocapacitance//EDLC

3.2.1. Metal Oxides (TiO_2, Nb_2O_5, etc.)//AC

Metal oxide electrodes usually show intercalation-pseudocapacitance-type electrochemical performance.[82,83] When metal oxides are utilized as anodes, they would show stable structures during (dis)charge, which contributes to long cycling performance.

TiO_2 cannot directly be used as anodes for AMHSs due to the sluggish ion kinetics and poor electron mobility.[65] However, heteroatom doping in metal oxides can effectively promote the performance. Bauer *et al.*[66] directly synthesized Mo or Nb doped TiO_2 via a continuous hydrothermal flow synthesis process. In the voltage range of 0.5–3.0 V and at power density of 180 W kg^{-1}, $Mo_{0.1}Ti_{0.9}O_2$/AC delivered an energy density of 51 W h kg^{-1}, and $Nb_{0.25}Ti_{0.7}O_2$/AC presented 45 W h kg^{-1}.

Here, carbon coating showed unique superiority.[67] Zhu *et al.*[68] fabricated a novel anode consisting of TiO_2, multiwalled carbon nanotubes (CNTs) and carbon electrospinning. The AC cathode was achieved from fallen leaves as biomass-derived AC (BAC) via a carbonized process. The SIHSs showed outstanding electrochemical performance in the voltage window of 1.0–4.0 V. After 350 cycles, it remained 98% retention capacity of 183 mA h g^{-1}, and the rate performance of TiO_2@CNT@C is also outstanding. As shown in Figure 7a, the SIHS exhibited an energy density of 81.2 W h kg^{-1} and high power density of 126 W kg^{-1} at 0.005 A g^{-1}. The SIHSs are almost on par with Li-ion batteries in energy density and supercapacitors in power density in Figure 7b. The long term cyclic tests in Figure 7c demonstrated the excellent reversibility with the capacitance loss of only 0.0029% per cycle during 5000 cycles. High surface area and abundant pores of cathodes contributed to the remarkable performance.

Nb_2O_5 has been utilized as the electrochemical energy storage material for several years; the intercalation-pseudocapacitance allowed the Li^+ reaction both in the bulk and on the surface, which make it an ideal material for AMHSs.[72–81] Deng *et al.*[69] reported Nb_2O_5 nanorod film anodes applied to LIHSs with AC cathodes. This was a binder-free material consisting of interconnected single-crystalline Nb_2O_5 nanorods, which contributed to high rate performance ((≈73% capacity retention with the rate increase from 0.5 to 20 C). The device delivered a high energy density of 95.55 W h kg^{-1} and a power density of

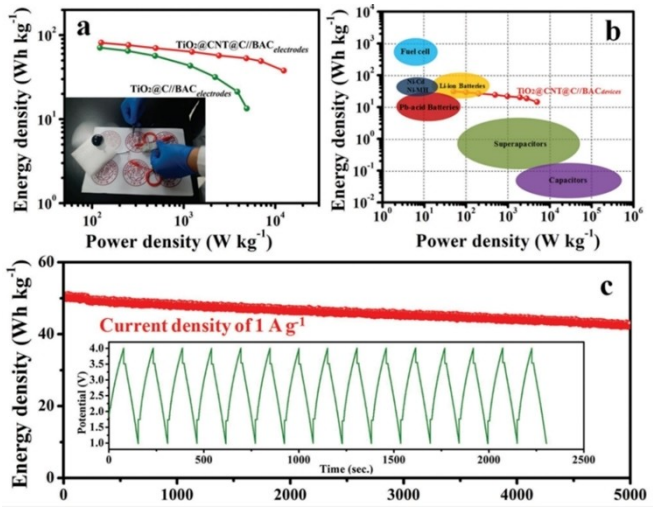

Figure 7. a) Ragone plots (energy density vs power density) of TiO_2@CNT@C//BAC and TiO_2@C//BAC full cells; b) device-based performance for the currently available energy-storage systems; c) long-term cycle performance at 1 A g^{-1} of TiO_2@CNT@C//BAC full cells. The inset in panel (a) shows the fan driving application. Reproduced from Ref. [68] with permission. Copyright (2017) Wiley-VCH.

5350.9 W kg^{-1}. Other modifications like free-standing *T*-Nb_2O_5/graphene composite papers[70] and 0D *T*-Nb_2O_5 embedded in carbon microtubes[71] were extensively studied.

3.3. Nernstian Storage//Pseudocapacitance

3.3.1. Nernstian Storage Materials//MXenes

MXenes are chemically derived from layered $M_{n+1}AX_n$ or MAX phases, where M is an early transition metal, A is an A-group element and X is C and/or N. These materials are a kind of 2D transition metal carbides, such as Ti_3C_2, Nb_2C and V_2C. They possess good lithium storage capability and are suitable for batteries and capacitors.

MXenes can be directly used in AMHSs. Li *et al.*[97] prepared accordion-like $Ti_3C_2T_x$ MXene via a simple combustion and acid treatment. When matched with commercial AC cathodes, the LIHSs gave a maximum energy density of 106 Wh kg^{-1} and power density of 5.2 kW kg^{-1}. When MXenes are assembled with carbon materials, the performance is improved. [98,99]

With surface modification, the performance will be largely improved. A typical MXene known as Ti_2C was utilized as anodes for SIHSs reported by Wang *et al.*[100] There are many surface functional groups such as OH, F and O for Ti_2C, and they would be denoted as T_x in Ti_2CT_x. This material showed good stability that after 100 cycles, the capacity retention is still over 81%. At 1.3 V versus Na/Na^+, it delivered a reversible capacity of 175 mAh g^{-1}, and no obvious change in the structure during charge-discharge processes. When combined with $Na_2Fe_2(SO_4)_3$ cathodes, the SIHSs achieved energy density of 320 and 260 Wh kg^{-1} at specific power density of 360 and 1,440 W kg^{-1}, respectively.

The pseudocapacitive charge storage mechanism contributed to the excellent electrochemical performance and liberated SIHSs from the trade-off between high energy and high power density. When heteroatoms were doped in MXenes, the performance could be significantly enhanced. Porous MXenes[101] are also suitable for AMHSs as anodes.

4. Carbon Materials

Carbon materials are usually used as capacitive materials for anodes or cathodes according to the relative potential of the other electrode. Commercial AC is the most widely applied capacitor-type electrode material due to its low cost and porous structure. The major flaw of capacitor-type electrode materials is low capacitance, which is the main reason for restricting the energy density of MHSs. In order to enhance the performance, many strategies are proposed such as constructing novel structures to expand surface area, and doping heteroatoms to enhance wettability and to provide pseudocapacitance.

4.1. Activated Carbon Materials

There are many merits of AC like the abundance of raw materials, low cost, high surface area and easy treatment which all contribute to the extensive use. Most capacitor-type electrodes are commercial AC. It could be obtained from biomass materials as well as polymers by high temperature treatment or acid/alkali activation.[104] Sun *et al.*[105] reported a biomass-derived AC from waste pomelo peels by a simple KOH activation process as cathodes, which was paired with Sn–C anodes. The obtained devices delivered high energy density of 195.7 Wh kg^{-1} and 84.6 Wh kg^{-1} at power densities of 731.25 W kg^{-1} and 24.375 kW kg^{-1}, respectively. Moreover, many biomass materials were explored to produce AC, such as coconut shells,[106] corncob,[107] rich husk,[108] prosopis juliflora,[109] peanut shells,[110] and pulping waste liquor .[111]

There are many strategies to enhance the capacitance of commercial AC to achieve better performance, such as surface functionalization.[112] Yu *et al.*[113] fabricated nitrogen-enriched mesoporous carbon nanosphere/graphene (N-GMCS) nanocomposites as cathodes for LIHSs and coupled with prelithiated microcrystalline graphite (PLMG) anodes (Figure 8). The triblock co-polymer F127 was used as the template to grow carbon nanospheres on graphene oxide (GO), and then treated under NH_3 atmosphere at 800 °C to realize N doping. The product possessed hierarchical porous structures with high electronic conductivity, which contributed to quick Faradaic reaction and high capacitance. This device delivered high energy density of 80 Wh kg^{-1} (68.6 Wh L^{-1}) and maximum power density of 352 kW kg^{-1}(292 kW L^{-1}). After 4000 cycles at 2 A g^{-1}, the capacity retention was 93% indicating high cycling stability. In addition, pyridine-derived porous nitrogen-doped carbon,[114] boron and nitrogen dual-doped 3D porous carbon nanofibers,[115] nitrogen and sulfur dual-doped 3D porous

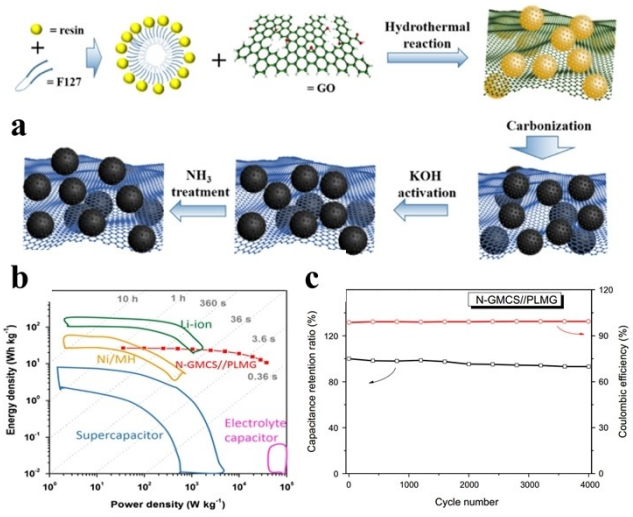

Figure 8. a) Schematic diagram for the synthesis of the N-GMCS nanocomposite. b) Device mass normalized Ragone plots of N-GMCS//PLMG hybrid devices and various commercial devices. c) Cycling stability of N-GMCS//PLMG hybrid devices at a current density of 2 A g^{-1} for 4000 cycles. Reproduced from Ref. [113] with permission. Copyright (2015) Elsevier.

carbon,[116] tubular mesoporous carbon,[117] polyaniline-derived carbon nanorods,[118] *etc.* have also been investigated. Those investigations provide new perspective in designing high-performance MHSs.

4.2. Carbon Nanostructured Materials

Carbon nanostructured materials consist of graphene,[119] graphdiyne[120] and CNTs.[121] Due to unique nanostructures, these materials possess many novel properties which can strongly improve the electrochemical performance for EES devices. Aravindan *et al.*[122] reported trigol-rGO (TRGO) as a capacitor-type cathode, via an ecofriendly trigol reduction process from graphene oxide. After paired with commercial $Li_4Ti_5O_{12}$, the device provided a long lifespan and a desirable energy density of 45 Wh kg^{-1}. This kind of materials could show both faradaic and non-faradaic mechanisms, but under most circumstances, they were more suitable for capacitor-type electrodes due to high specific surface area.

5. Electrolytes

The electrolytes are generally classified into four kinds: aqueous, organic, ionic liquids and solid electrolytes. They play a significant part in the electrochemical performance of EES systems. Firstly, they are burdened with the ion transportation between the paired electrodes, which determine the power magnitude (output rate of energy). Moreover, their intrinsic resistance and operation voltage range have large influence on the capacity or energy density. It is essential for researchers to pay close attention to make progress in electrolytes.

5.1. Organic Electrolytes

The widely applicable organic electrolytes are organic salts such as $LiPF_6$ and $NaClO_4$ dissolved in organic solvents such as ethylene carbonate and ethyl methyl carbonate.[123] Organic electrolytes have a wide voltage range, which can effectively enhance the energy density and capacity, and the performance at high voltage. Most of them have high ion conductivity which can provide high power density. But the defects are fatal that organic electrolytes have inferior thermal stability which could cause decomposition and are inflammable and toxic, and people make great efforts on the solution.[124]

While organic electrolytes were applied, side reactions often happened during the (dis)charge process. The harmful interaction between electrodes and electrolytes is inevitable, such as decomposition, corrosion and unnecessary redox reactions, which could not only cause severe safety problems, but worsen the electrochemical performance. It is efficient to alleviate those problems by adding a spot of substances into electrolytes, which were called "additives". They are capable of stabilizing the electrolyte, making them heat resisting and decreasing the generation of harmful gases to enhance the cycle ability. Boltersdorf *et al.*[125] explored vinylene carbonate (VC) or tris(trimethylsilyl) phosphate (TMSP) as additives in a LIHSs consisting of prelithiated hard carbon anodes and AC cathodes (Figure 9). When the additive was 1% TMSP in the electrolyte of 1 M $LiPF_6$ ethylene carbonate (EC): dimethyl carbonate (DMC), the device exhibited outstanding performance: a high energy density of 56.8 Wh kg^{-1}, and 70% capacity retention after 500 cycles at 65 °C, compared with 33.2 Wh kg^{-1} and 44.3% without any additive, respectively. That demonstrated that TMSP additive could be effective to maintain the performance stability at high temperatures, indicating the inhibition of electrolyte decomposition and gas production.

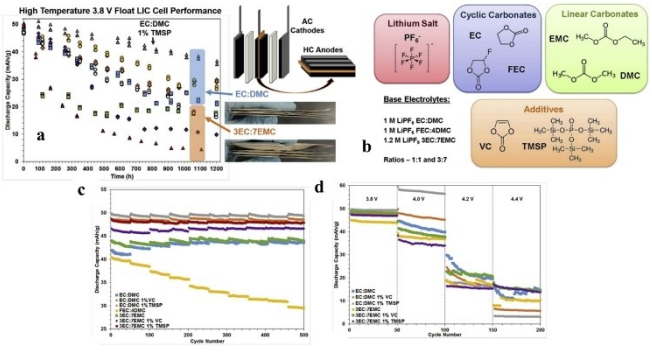

Figure 9. The three-layer LIHS cells of EC: DMC and 3EC: 7EMC (Ethyl methyl carbonate) based electrolytes with various additives of: a) high temperature float at 3.8 V and schematic of comparing the capacity retention; b) molecular diagram; c) the cycle life performance at room temperature shown by alternating float at 3.8 V; d) performance at increasing upper cutoff potentials. Reproduced from Ref. [125] with permission. Copyright (2017) Elsevier.

5.2. Aqueous Electrolytes

The aqueous electrolytes (the aqueous solutions of H_2SO_4, KCl, *etc.*) are used in AMHSs. They are low cost, abundant and easy to manufacture. But the potential window is restricted because of the electrolysis of water, meaning that only in low voltages can these devices work normally. This defect severely limits the energy density and the further application of aqueous electrolytes.

5.3. Ionic Liquid Electrolytes

Compared with the above two kinds of electrolytes, ionic liquid electrolytes show not merely incombustible and nontoxic property but also wider electrochemical window. Ionic liquids composed of anions and cations are molten salts at room temperature. Due to high viscosity, some kinds of ionic liquids have low ionic conductivity. Moreover, the interface passivation and unstable SEI films between electrodes and ionic liquids limit their further applications on electrochemical energy storage systems.

5.4. Quasi-Solid-State Electrolytes

Traditional liquid electrolytes suffer from safety problems in batteries or supercapacitors. In recent years, various accidents have occurred to lithium-ion batteries/capacitors from time to time, making the safety of lithium-ion batteries/capacitors questioned. Overcharge, overheating, and mechanical damage would cause spontaneous combustion or explosion. People have put forward higher and stricter requirement for the electrochemical performance and safety of lithium-ion batteries. However, it is a difficult problem to solve because the commercial electrolytes for lithium-ion batteries/capacitors are flammable organic liquids, with poor thermal stability and low ignition point. At present, the methods, such as strengthening safety management and developing flame-retardant materials, have not substantially solved the problem from the inside, and quasi-solid-state metal-ion capacitors with gel polymers can alleviate those problems. This idea was first applied in lithium/sodium ion capacitors and achieved some satisfied results. [126]

For LIHSs, Yu *et al.* [127] reported a novel electrolyte based on poly(vinylidene fluoride-co-hexafluoropropylene) (P(VDF-HFP)) membrane modified by Al_2O_3 nanoparticles. They chose folded and crumpled morphology graphene nanosheets (GNS) as cathodes, and quasi-layered titanate hydrates (Q-TH) deriving from the dehydration-induced structural rearrangement of Ti–O octahedra as anodes. This quasi-solid-state LIHSs delivered a high energy density of 116 Wh kg^{-1}, as well as impressive cycle ability of 86% capacity retention after 300 cycles. Via first-principles computations, four possible lithium diffusion paths are proposed in Figure 10c. Except polyoxometalates, metal oxides such as TiO_2[128] were also applied in quasi-solid-state LIHSs.

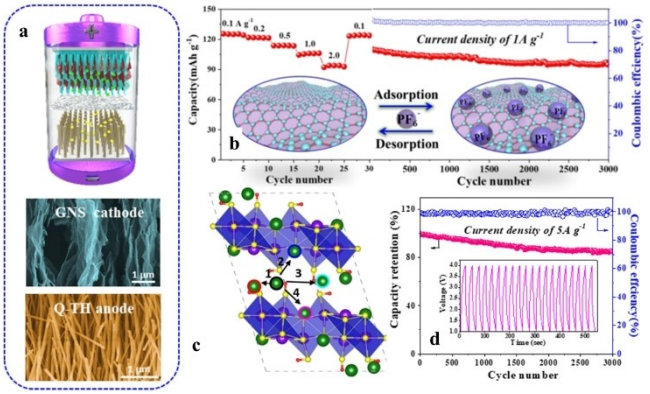

Figure 10. a) Schematic illustration of Q-TH//GNS hybrid capacitors; b) Rate capability and cycle performance at 1.0 A g^{-1} of the GNS cathode; c) Illustration of the Li^+ diffusion paths in the bulk of Q-TH; d) Cycle stability of Q-TH//GNS LIC at 5.0 A g^{-1}. Reproduced from Ref. [127] with permission. Copyright (2019) Elsevier.

For SIHSs, a quasi-solid-state SHIS was fabricated by Li *et al.*,[129] which consisted of an anode of urchin-like $Na_2Ti_3O_7$ and a carbon cathode derived from peanut shells. The electrolyte was a gel polymer that could conduct sodium ions. This device exhibited energy densities of 111.2 Wh kg^{-1} and 33.2 Wh kg^{-1} at power densities of 0.8 kW kg^{-1} and 1.12 kW kg^{-1}, respectively. Meanwhile, the cycling performances are also impressive (86% capacity retention over 3000 cycles).

6. New Techniques on Hybrid Supercapacitors

Many efforts have been made to construct novel capacitors and develop electrode treatment. Although some strategies are in their early stage, they still show high promising vista, which could give researchers more ideas.

6.1. Symmetric Metal-Ion Hybrid Supercapacitors

Under different conditions, one material can exhibit not only chemical-insertion battery-type behaviors, but also physical-adsorption capacitor-type ones. This fact makes symmetric metal ion hybrid supercapacitors possible. The compatibility of two types of electrodes significantly affects the performances of hybrid supercapacitors. However, two identical electrodes in symmetric metal ion hybrid supercapacitors can availably reduce the possibility of this problem.

Carbon materials doped with heteroatoms can also be used as identical electrodes. Yan *et al.*[130] utilized porous and S/N co-doped carbon nanospheres as both anodes and cathodes. The pore volume is 1.23 cm^3 g^{-1}, the S doping rate is 10.8 at%, and the surface area is 1006.7 cm^3 g^{-1}, which can effectively shorten the path length for both electrons and Li^+ ions, improve its electrical conductivity and provide abundant active sites. Benefiting from these, the device presented energy densities of 222.97 and 8.3 Wh kg^{-1} at power density of 0.273 and even 93.8 kW kg^{-1}, respectively. When cycled for 10000 cycles at a

power density of 5 kW kg^{-1}, it showed 74% capacity retention of 101.4 Wh kg^{-1}. Those results indicated that identical electrodes in one device are promising for large electrochemical energy storage systems.

Moreover, Chen *et al.*[131] fabricated two identical $Na_{0.44}MnO_2$ nanorods as both anodes and cathodes. The unique structure significantly reduced the Na^+ diffusion barrier and facilitate Na^+ (de)intercalation. This symmetric SIHSs delivered an energy density of 27.9 Wh kg^{-1} as well as a high power density of 2432.7 W kg^{-1}. After 5000 cycles at 1.8 A g^{-1} (30 C), it showed great stability of 85.2% capacity retention.

6.2. New Prelithiation/Presodiation Methods

For some type MHSs, there is a problem of the lack of metal sources in the whole system. So, the additional supply for metal elements is need. Prelithiation/presodiation can provide extra metal resources. At the meantime, it will keep a much lower potential for anodes, leading to a wide voltage window as well as high operation voltage. Moreover, it has effects on the formation on solid electrolyte interface (SEI) films and extra metal elements will thicken the film and further influences the ion diffusion and cycle stability.

The traditional way to prelithiation/presodiation for L/SIHSs is assembling materials with metallic lithium/sodium as half cells, which is in lack of convenience because of an additional re-assemble step and the level of prelithiation/presodiation is hard to precisely define. However, this traditional method also has some advantages such as a stable and uniform SEI films. Recently, this process has tended to utilize metal salts as the resource for MHSs, such as Li_6CoO_4[132] and Li_2S.[133] But these prelithiated materials as extra sacrificial matters do have significant influence on the whole system due to their high potential of lithium ion extraction, which can destroy electrodes or electrolytes. Sun *et al.*[134] reported a high-efficiency sacrificial prelithiation that Li_3N is employed as a sacrificial prelithiation material with a low prelithiation potential of 4.1 V. LIHSs with AC cathodes and soft carbon anodes prelithiated by Li_3N displayed satisfied performance. It delivered an energy density of 74.7 Wh kg^{-1} and a power density of 12.9 kW kg^{-1}, and long lifespan was achieved with 91% capacity retention after 10000 cycles at 0.5 A g^{-1}. Some materials can be bifunctional as both prelithiation reagent and pseudocapacitive electrode, such as Li_6CoO_4.[135] Zou *et al.*[136] proposed a novel approach to realize in situ presodiation via voltage-induced organic sodium salts ($Na_2C_6O_2$ and $Na_2C_6H_2O_6$) (Figure 11). These salts were abundant, cheap and environmentally friendly. The high irreversibility could provide sufficient sodium sources for anodes. The assembled devices with successful presodiation exhibit outstanding electrochemical performances, proving that no negative effect was introduced by this new method.

An alternative way was proposed. There is pre-set lithium/sodium in AMHSs devices and an extra cycle is operated to consume Li/Na metal. When the prelithiation/presodiation is done, the device can be cycled. This method avoids a re-assembly process despite a long lithiation/sodiation time.

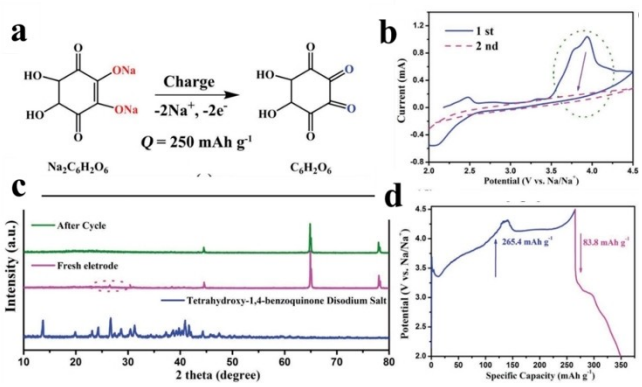

Figure 11. a) Scheme of the desodiation of $Na_2C_6H_2O_6$ cathode. b) CV curves at 5 mV s^{-1} and c) ex situ XRD patterns of $Na_2C_6H_2O_6$ cathode. d) Galvanostatic charge/ discharge curves at 0.1 C of $Na_2C_6H_2O_6$ cathode. Reproduced from Ref. [136] with permission. Copyright (2020) Wiley-VCH.

6.3. Protection of Metal Anodes

Ideally, a metal is the best anode choice for any metal ion EES system. But due to various reasons such as side reactions with electrolytes, the metal is not able to be applied directly or exhibits unsatisfied performance. The protection of metal anodes has attracted attention in recent years, and many strategies are proposed to solve this problem. The common way is introducing a protective film on the surface of metals.[137] For LIHSs, Zhan *et al.*[138] proposed a novel method to construct a water-proof interlayer to protect lithium anodes by introducing garnet solid-state composite electrolytes with high compactness. With high lithium ion conductivity, the cubic phase garnet $Li_{6.75}La_3Zr_{1.75}Nb_{0.25}O_{12}$ containing Li_3BO_3 via a traditional solid-state reaction was used as the separator between lithium metal anodes and electrolytes. With assembled with AC cathodes, the devices could be operated normally at a high voltage of 4.0 V with a wide voltage window of 1.8 V, and showed outstanding performance as a high specific energy of 228.9 Wh (kg-carbon)$^{-1}$ at a specific power of 1343.2 W (kg-carbon)$^{-1}$.

7. Conclusions and Perspectives

Alkali metal-ion hybrid supercapacitors featuring the integration of high-energy battery-type electrodes and high-power capacitor-type electrodes have caught vast attention. For the past a few years, the development of hybrid supercapacitors mainly focuses on the enhancement of energy and power density. However, assembling hybrid supercapacitors is not meaning just putting two kinds of electrodes together into a device, and matching two kinds of materials is not an easy task due to substantial incompatibility. Up to now, the electrochemical performances of AMHSs are not so amazing, and significant improvements are still needed.

Widening voltage window is the core way to obtain larger capacity. Traditional AMHSs show a normal voltage range of 0–3 V, which is not wide enough to support high energy density.

Alkali metals have lower potential and may be the best choice to get larger window, but they are restricted by many factors and need additional protection strategies. While with pre-lithiation/presodiation, the potential of general anodes will be effectively lowered even close to alkali metal level and increase the window to 0–4 V or higher.

Facilitating the diffusion of ions in the bulk and surface is fundamental to attain improved kinetics. The fast charge/discharge response is depended on the diffusion control and the common method is to shorten the pathway of ions. Nanosized particles of battery-type materials can provide fast surface de/intercalation and avoid sluggish kinetics of diffusion in the bulk, and the large surface areas also help maintain large capacity. Combining with other strategies, it is possible to assemble a perfect material such as highly dispersed nanosized particles in heteroatom-doped porous carbon with 3D hierarchical architectures.

It is not easy to get a comparable LIB and supercapacitor level device. Relatively limited power proficiency and insufficient energy density of AMHSs are the main challenges. Firstly, it is the intrinsic nature of AMHSs that restricts their upper limit, and traditional battery-type electrodes and capacitor-type electrodes have their ceiling and hinder the breakthrough. New systems of AMHSs from lithium to potassium with unique merits are designed to endow these devices with better performances, lower cost and higher kinetics. Another is the essential difficulty of matching two different electrodes. The poor compatibility has no method so far to be solved thoroughly unless identical electrodes are used. To match the kinetics as well as energy density, both electrodes should be modified scientifically and the mass of each active material needs to be evaluated charily. For a few years, the application of hybrid supercapacitors mainly focuses on portable devices and wearable electronic products, indicating that the size of hybrid supercapacitors tends to be smaller and micro devices become mainstream.[139,140] but this is far from enough. Further studies on technologies and materials of AMHSs are still imperative to board their level up to a new degree.

Acknowledgements

This work was supported by National Key R&D Program of China (2016YFA0200200).

Conflict of Interest

The authors declare no conflict of interest.

Keywords: alkali metal-ion hybrid supercapacitors · electrodes · prelithiation · electric double-layer capacitance · pseudocapacitance · Nernstian storage

[1] A. Muzaffar, M. B. Ahamed, K. Deshmukh, J. Thirumalai, *Renewable Sustainable Energy Rev.* **2019**, *101*, 123–145.
[2] V. Aravindan, J. Gnanaraj, Y. Lee, S. Madhavi, *Chem. Rev.* **2014**, *114*, 11619–11635.
[3] Z. Yang, J. Tian, Z. Yin, C. Cui, W. Qian, F. Wei, *Carbon* **2019**, *141*, 467–480.
[4] A. Afif, S. M. Rahman, A. Tasfiah Azad, J. Zaini, M. A. Islan, A. K. Azad, *J. Energy Storage* **2019**, *25*, 100852.
[5] L. Dong, W. Yang, W. Yang, Y. Li, W. Wu, G. Wang, *J. Mater. Chem. A* **2019**, *7*, 1381–13832.
[6] J. Xu, B. Gao, K. Huo, P. K. Chu, *J. Nanosci. Nanotechnol.* **2020**, *20*, 2652–2667.
[7] Y. Zhang, J. Jiang, Y. An, L. Wu, H. Dou, J. Zhang, Y. Zhang, S. Wu, M. Dong, X. Zhang, Z. Guo, *ChemSusChem* **2020**, *13*, 2522–2539.
[8] A. Le Comte, Y. Reynier, C. Vincens, C. Leys, P. Azaïs, *J. Power Sources* **2017**, *363*, 34–43.
[9] G. Z. Chen, *Curr. Opin. Electrochem.* **2020**, *21*, 358–367.
[10] J. Zheng, Y. Yang, X. Fan, G. Ji, X. Ji, H. Wang, S. Hou, M. R. Zachariah, C. Wang, *Energy Environ. Sci.* **2019**, *12*, 615–623.
[11] G. Haxel, J. B. Hedrick, G. J. Orris, G. S. U. S. 2002. *Rare Earth Elements: Critical Resources for High Technology* ***2002****, Report 2327–6932.*
[12] H. Helmholtz, *Ann. Phys.* **1879**, *243*, 337–382.
[13] M. Gouy, *J. Phys. Theor. Appl.* **1910**, *9*, 457–468.
[14] D. L. Chapman, *Philos. Mag.* **1913**, *25*, 475–481.
[15] O. Stern, *Elektrochem. Angew. Phys. Chem.* **1924**, *30*, 508–516.
[16] S. Fleischmann, J. B. Mitchell, R. Wang, C. Zhan, D. E. Jiang, V. Presser, V. Augustyn, *Chem. Rev.* **2020**, *120*, 6738–6782.
[17] D. C. Grahame, *J. Am. Chem. Soc.* **1941**, *63*, 1207–1215.
[18] B. E. Conway, *Trans. Faraday Soc.* **1962**, *58*, 2493–2509.
[19] H. Gu, Y. Zhu, J. Yang, J. Wei, Z. Zhou, *ChemNanoMat* **2016**, *2*, 578–587.
[20] M. Yang, Z. Zhou, *Adv. Sci.* **2017**, *4*, 1600408.
[21] M. Yang, Y. Zhong, J. Bao, X. Zhou, J. Wei, Z. Zhou, *J. Mater. Chem. A* **2015**, *3*, 11387–11394.
[22] M. Okubo, E. Hosono, J. Kim, M. Enomoto, N. Kojima, T. Kudo, H. Zhou, I. Honma, *J. Am. Chem. Soc.* **2007**, *129*, 7444–7452.
[23] K. Naoi, S. Ishimoto, Y. Isobe, S. Aoyagi, *J. Power Sources* **2010**, *195*, 6250–6254.
[24] Y. Zhang, Z. Zhang, Y. Tang, D. Jia, Y. Huang, W. Pang, Z. Guo, Z. Zhou, *Adv. Funct. Mater.* **2019**, *29*, 1807895.
[25] M. Secchiaroli, G. Giuli, B. Fuchs, R. Marassi, M. Wohlfahrt-Mehrens, S. Dsoke, *J. Mater. Chem. A* **2015**, *3*, 11807–11816.
[26] H. Gu, L. Kong, H. Cui, X. Zhou, Z. Xie, Z. Zhou, *J. Energy Chem.* **2019**, *28*, 79–84.
[27] H. V. Ramasamy, B. Senthilkumar, P. Barpanda, Y. Lee, *Chem. Eng. J.* **2019**, *368*, 235–243.
[28] A. Shellikeri, S. Yturriaga, J. S. Zheng, W. Cao, M. Hagen, J. A. Read, T. R. Jow, J. P. Zheng, *J. Power Sources* **2018**, *392*, 285–295.
[29] H. Gao, J. Wang, R. Zhang, L. Wu, C. Tao, G. Deng, *Mater. Res. Express* **2019**, *6*, 45509.
[30] B. Zhuang, Z. Guo, W. Chu, Z. Cao, T. Bold, Y. Gao, *Electrochim. Acta* **2018**, *283*, 1589–1599.
[31] M. Hu, J. P. Wei, L. Y. Xing, Z. Zhou, *J. Power Sources* **2013**, *222*, 373–378.
[32] L. Xu, S. Wang, X. Zhang, T. He, F. Lu, H. Li, J. Ye, *Appl. Surf. Sci.* **2018**, *428*, 977–985.
[33] S. Lee, T. Lee, *Int. J. Hydrogen Energy* **2018**, *43*, 15365–15369.
[34] L. Chen, W. Zhai, L. Chen, D. Li, X. Ma, Q. Ai, X. Xu, G. Hou, L. Zhang, J. Feng, P. Si, L. Ci, *J. Power Sources* **2018**, *392*, 116–122.
[35] L. Chen, D. Li, X. Zheng, L. Chen, Y. Zhang, Z. Liang, J. Feng, P. Si, J. Lou, L. Ci, *J. Electroanal. Chem.* **2019**, *842*, 74–81.
[36] K. Wasiński, P. Półrolniczak, M. Walkowiak, *Electrochim. Acta* **2018**, *259*, 850–854.
[37] K. Kaliyappan, Z. Chen, *Nano Energy* **2018**, *48*, 107–116.
[38] S. R. Sivakkumar, A. G. Pandolfo, *Electrochim. Acta* **2012**, *65*, 280–287.
[39] J. Zhang, X. Liu, J. Wang, J. Shi, Z. Shi, *Electrochim. Acta* **2016**, *187*, 134–142.
[40] K. Kuratani, M. Yao, H. Senoh, N. Takeichi, T. Sakai, T. Kiyobayashi, *Electrochim. Acta* **2012**, *76*, 320–325.
[41] J. Chen, B. Yang, H. Hou, H. Li, L. Liu, L. Zhang, X. Yan, *Adv. Energy Mater.* **2019**, *9*, 1803894.
[42] H. Konno, T. Kasashima, K. Azumi, *J. Power Sources* **2009**, *191*, 623–627.
[43] B. Li, S. Li, Y. Jin, J. Zai, M. Chen, A. Nazakat, P. Zhan, Y. Huang, X. Qian, *J. Mater. Chem. A* **2018**, *6*, 21098–21103.
[44] F. Sun, X. Liu, H. B. Wu, L. Wang, J. Gao, H. Li, Y. Lu, *Nano Lett.* **2018**, *18*, 3368–3376.

[45] F. Zhang, W. Zhang, J. Guo, Y. Lei, M. A. Dar, Z. Almutairi, H. N. Alshareef, *Energy Technol.* **2020**, 8, 2000193.
[46] M. Liu, Z. Zhang, M. Dou, Z. Li, F. Wang, *Carbon* **2019**, *151*, 28–35.
[47] C. Li, X. Zhang, K. Wang, X. Sun, Y. Ma, *Carbon* **2018**, *140*, 237–248.
[48] Y. Luan, R. Hu, Y. Fang, K. Zhu, K. Cheng, J. Yan, K. Ye, G. Wang, D. Cao, *Nano-Micro Lett.* **2019**, *11*, 30.
[49] T. Liang, H. Wang, R. Fei, R. Wang, B. He, Y. Gong, C. Yan, *Nanoscale* **2019**, *11*, 20715–20724.
[50] J. Su, Y. Wu, C. Huang, Y. Chen, H. Cheng, P. Cheng, C. Hsieh, S. Lu, *Chem. Eng. J.* **2020**, *396*, 125314.
[51] J. Jiang, Y. Zhang, Z. Li, Y. An, Q. Zhu, Y. Xu, S. Zang, H. Dou, X. Zhang, *J. Colloid Interface Sci.* **2020**, *567*, 75–83.
[52] Y. Sun, J. Ma, X. Yang, L. Wen, W. Zhou, J. Geng, *J. Mater. Chem. A* **2020**, *8*, 62–68.
[53] Y. Xu, J. Jiang, Z. Li, Z. Yang, Y. Zhang, Y. An, Q. Zhu, H. Dou, X. Zhang, *J. Colloid Interface Sci.* **2020**, *55*, 13127–13140.
[54] Y. An, S. Chen, M. Zou, L. Geng, X. Sun, X. Zhang, K. Wang, Y. Ma, *Rare Met.* **2019**, *38*, 1113–1123.
[55] P. Wang, B. Yang, G. Zhang, L. Zhang, H. Jiao, J. Chen, X. Yan, *Chem. Eng. J.* **2018**, *353*, 453–459.
[56] D. Qiu, A. Gao, Z. Xie, L. Zheng, C. Kang, Y. Li, N. Guo, M. Li, F. Wang, R. Yang, *ACS Appl. Mater. Interfaces* **2018**, *10*, 44483–44493.
[57] R. Yan, E. Josef, H. Huang, K. Leus, M. Niederberger, J. P. Hofmann, R. Walczak, M. Antonietti, M. Oschatz, *Adv. Funct. Mater.* **2019**, *29*, 1902858.
[58] G. Lu, H. Wang, Y. Zheng, H. Zhang, Y. Yang, J. Shi, M. Huang, W. Liu, *Electrochim. Acta* **2019**, *319*, 541–551.
[59] D. Li, C. Ye, X. Chen, S. Wang, H. Wang, *J. Power Sources* **2018**, *382*, 116–121.
[60] L. Jin, X. Guo, R. Gong, J. Zheng, Z. Xiang, C. Zhang, J. P. Zheng, *Energy Storage Mater.* **2019**, *23*, 409–417.
[61] Y. Ding, B. Yang, J. Chen, L. Zhang, J. Li, Y. Li, X. Yan, *Sci. China Mater.* **2018**, *61*, 285–295.
[62] K. Liao, H. Wang, L. Wang, D. Xu, M. Wu, R. Wang, B. He, Y. Gong, X. Hu, *Nanoscale Adv.* **2019**, *1*, 746–756.
[63] Y. Ding, Y. Li, J. Li, X. Yan, *Chin. Chem. Lett.* **2019**, *9*, 2219–2224.
[64] J. Kan, H. Wang, H. Zhang, J. Shi, W. Liu, D. Li, G. Dong, Y. Yang, R. Gao, *Electrochim. Acta* **2019**, *304*, 192–201.
[65] H. Wang, C. Guan, X. Wang, H. J. Fan, *Small* **2015**, *11*, 1470–1477.
[66] D. Bauer, A. J. Roberts, N. Matsumi, J. A. Darr, *Nanotechnology* **2017**, *28*, 195403.
[67] H. Kim, D. Mhamane, M. Kim, H. Roh, V. Aravindan, S. Madhavi, K. C. Roh, K. Kim, *J. Power Sources* **2016**, *327*, 171–177.
[68] Y. Zhu, L. Yang, J. Sheng, Y. Chen, H. Gu, J. Wei, Z. Zhou, *Adv. Energy Mater.* **2017**, *7*, 1701222.
[69] B. Deng, T. Lei, W. Zhu, L. Xiao, J. Liu, *Adv. Funct. Mater.* **2018**, *28*, 1704330.
[70] L. Kong, C. Zhang, J. Wang, W. Qiao, L. Ling, D. Long, *ACS Nano* **2015**, *9*, 11200–11208.
[71] S. Hemmati, G. Li, X. Wang, Y. Ding, Y. Pei, A. Yu, Z. Chen, *Nano Energy* **2019**, *56*, 118–126.
[72] S. Fu, Q. Yu, Z. Liu, P. Hu, Q. Chen, S. Feng, L. Mai, L. Zhou, *J. Mater. Chem. A* **2019**, *7*, 11234–11240.
[73] R. Bi, N. Xu, H. Ren, N. Yang, Y. Sun, A. Cao, R. Yu, D. Wang, *Angew. Chem. Int. Ed.* **2020**, *59*, 4865–4868.
[74] Y. Li, R. Wang, W. Zheng, Q. Zhao, S. Sun, G. Ji, S. Li, X. Fan, C. Xu, *Mater. Technol.* **2020**, 1–10.
[75] V. Ojha, K. Kato, M. A. Kabbani, G. Babu, P. M. Ajayan, *ChemistrySelect* **2019**, *4*, 1098–1102.
[76] J. Zhang, H. Zhang, Y. Zhang, J. Zhang, H. He, X. Zhang, J. Shim, S. Zhang, *Electrochim. Acta* **2019**, *313*, 532–543.
[77] X. Jiao, Q. Hao, X. Xia, Z. Wu, W. Lei, *Chem. Commun. (Cambridge, U. K.)* **2019**, 55, 2692–2695.
[78] S. Jiang, S. Dong, L. Wu, Z. Chen, L. Shen, X. Zhang, *J. Electroanal. Chem.* **2019**, *842*, 82–88.
[79] D. Li, J. Shi, H. Liu, C. Liu, G. Dong, H. Zhang, Y. Yang, G. Lu, H. Wang, *Sustainable Energy Fuels* **2019**, *3*, 1055–1065.
[80] S. Hemmati, G. Li, X. Wang, Y. Ding, Y. Pei, A. Yu, Z. Chen, *Nano Energy* **2019**, *56*, 118–126.
[81] Y. Lian, D. Wang, S. Hou, C. Ban, J. Zhao, H. Zhang, *Electrochim. Acta* **2020**, *330*, 135204.
[82] J. Dong, Y. Jiang, Q. Wei, S. Tan, Y. Xu, G. Zhang, X. Liao, W. Yang, Q. Li, Q. An, L. Mai, *Small* **2019**, *15*, 1900379.
[83] B. Huang, S. Liu, X. Zhao, Y. Li, J. Yang, Q. Chen, S. Xiao, W. Zhang, H. Wang, G. Cao, *Sci. China Mater.* **2021**, *64*, 85–95.
[84] R. Wang, S. Wang, D. Jin, Y. Zhang, Y. Cai, J. Ma, L. Zhang, *Energy Storage Mater.* **2017**, *9*, 195–205.
[85] C. Miao, X. Xiao, Y. Gong, K. Zhu, K. Cheng, K. Ye, J. Yan, D. Cao, G. Wang, P. Xu, *ACS Appl. Mater. Interfaces* **2020**, *12*, 9365–9375.
[86] Z. Xia, H. Sun, X. He, Z. Sun, C. Lu, J. Li, Y. Peng, S. Dou, J. Sun, Z. Liu, *Nano Energy* **2019**, *60*, 385–393.
[87] J. Ge, B. Wang, J. Wang, Q. Zhang, B. Lu, *Adv. Energy Mater.* **2019**, *10*, 1903277.
[88] P. Wang, R. Wang, J. Lang, X. Zhang, Z. Chen, X. Yan, *J. Mater. Chem. A* **2016**, *4*, 9760–9766.
[89] M. Liu, L. Zhang, P. Han, X. Han, H. Du, X. Yue, Z. Zhang, H. Zhang, G. Cui, *Part. Part. Syst. Charact.* **2015**, *32*, 1006–1011.
[90] G. Wang, C. Lu, X. Zhang, B. Wan, H. Liu, M. Xia, H. Gou, G. Xin, J. Lian, Y. Zhang, *Nano Energy* **2017**, *36*, 46–57.
[91] W. Zhu, S. A. El-Khodary, S. Li, B. Zou, R. Kang, G. Li, D. H. L. Ng, X. Liu, J. Qiu, Y. Zhao, Y. Huang, J. Lian, H. Li, *Chem. Eng. J.* **2020**, *385*, 123881.
[92] V. Aravindan, J. Sundaramurthy, A. Jain, P. S. Kumar, W. C. Ling, S. Ramakrishna, M. P. Srinivasan, S. Madhavi, *ChemSusChem* **2014**, *7*, 1858–1863.
[93] J. Yin, L. Qi, H. Wang, *ACS Appl. Mater. Interfaces* **2012**, *4*, 2762–2768.
[94] S. Dong, L. Shen, H. Li, G. Pang, H. Dou, X. Zhang, *Adv. Funct. Mater.* **2016**, *26*, 3703–3710.
[95] S. Dong, Z. Li, Z. Xing, X. Wu, X. Ji, X. Zhang, *ACS Appl. Mater. Interfaces* **2018**, *10*, 15542–15547.
[96] H. Chen, Y. Wu, J. Duan, R. Zhan, W. Wang, M. Wang, Y. Chen, M. Xu, S. Bao, *ACS Appl. Mater. Interfaces* **2019**, *11*, 42197–42205.
[97] C. Li, X. Zhang, K. Wang, X. Sun, Y. Ma, *Chin. Chem. Lett.* **2020**, *31*, 1009–1013.
[98] P. Yu, G. Cao, S. Yi, X. Zhang, C. Li, X. Sun, K. Wang, Y. Ma, *Nanoscale* **2018**, *10*, 5906–5913.
[99] Z. Li, G. Chen, J. Deng, D. Li, T. Yan, Z. An, L. Shi, D. Zhang, *ACS Sustainable Chem. Eng.* **2019**, *7*, 15394–15403.
[100] X. Wang, S. Kajiyama, H. Iinuma, E. Hosono, S. Oro, I. Moriguchi, M. Okubo, A. Yamada, *Nat. Commun.* **2015**, *6*, 6544.
[101] F. Ming, H. Liang, W. Zhang, J. Ming, Y. Lei, A. Emwas, H. N. Alshareef, *Nano Energy* **2019**, *62*, 853–860.
[102] C. Cui, H. Wang, M. Wang, X. Ou, Z. Wei, J. Ma, Y. Tang, *Small* **2019**, *15*, 1902659.
[103] J. Lang, J. Li, X. Ou, F. Zhang, K. Shin, Y. Tang, *ACS Appl. Mater. Interfaces* **2019**, *12*, 2424–2431.
[104] S. Natarajan, Y. S. Lee, V. Aravindan, *Chem. Asian J.* **2019**, *14*, 936–951.
[105] F. Sun, J. Gao, Y. Zhu, X. Pi, L. Wang, X. Liu, Y. Qin, *Sci. Rep.* **2017**, *7*, 40990.
[106] A. Jain, V. Aravindan, S. Jayaraman, P. S. Kumar, R. Balasubramanian, S. Ramakrishna, S. Madhavi, M. P. Srinivasan, *Sci. Rep.* **2013**, *3*, 3002.
[107] B. Li, H. Zhang, D. Wang, H. Lv, C. Zhang, *RSC Adv.* **2017**, *7*, 37923–37928.
[108] K. Chen, D. Xue, *Chin. J. Chem.* **2017**, *35*, 861–866.
[109] P. Sennu, V. Aravindan, M. Ganesan, Y. Lee, Y. Lee, *ChemSusChem* **2016**, *9*, 849–854.
[110] J. Chen, X. Zhou, C. Mei, J. Xu, S. Zhou, C. Wong, *J. Power Sources* **2017**, *342*, 48–55.
[111] L. Jin, R. Gong, W. Zhang, Y. Xiang, J. Zheng, Z. Xiang, C. Zhang, Y. Xia, J. P. Zheng, *J. Mater. Chem. A* **2019**, *7*, 8234–8244.
[112] C. Liu, B. B. Koyyalamudi, L. Li, S. Emani, C. Wang, L. L. Shaw, *Carbon* **2016**, *109*, 163–172.
[113] X. Yu, C. Zhan, R. Lv, Y. Bai, Y. Lin, Z. Huang, W. Shen, X. Qiu, F. Kang, *Nano Energy* **2015**, *15*, 43–53.
[114] H. Wang, Y. Zhang, H. Ang, Y. Zhang, H. T. Tan, Y. Zhang, Y. Guo, J. B. Franklin, X. L. Wu, M. Srinivasan, H. J. Fan, Q. Yan, *Adv. Funct. Mater.* **2016**, *26*, 3082–3093.
[115] Q. Xia, H. Yang, M. Wang, M. Yang, Q. Guo, L. Wan, H. Xia, Y. Yu, *Adv. Energy Mater.* **2017**, *7*, 1701336.
[116] X. Tang, H. Liu, X. Guo, S. Wang, W. Wu, A. K. Mondal, C. Wang, G. Wang, *Mater. Chem. Front.* **2018**, *2*, 1811–1821.
[117] W. Qu, F. Han, A. Lu, C. Xing, M. Qiao, W. Li, *J. Mater. Chem. A* **2014**, *2*, 6549.
[118] C. Liu, Q. Ren, S. Zhang, B. Yin, L. Que, L. Zhao, X. Sui, F. Yu, X. Li, D. Gu, Z. Wang, *Chem. Eng. J.* **2019**, *370*, 1485–1492.
[119] T. Liang, H. Wang, D. Xu, K. Liao, R. Wang, B. He, Y. Gong, C. Yan, *Nanoscale* **2018**, *10*, 17814–17823.
[120] H. Du, H. Yang, C. Huang, J. He, H. Liu, Y. Li, *Nano Energy* **2016**, *22*, 615–622.

[121] A. Byeon, A. M. Glushenkov, B. Anasori, P. Urbankowski, J. Li, B. W. Byles, B. Blake, K. L. Van Aken, S. Kota, E. Pomerantseva, J. W. Lee, Y. Chen, Y. Gogotsi, *J. Power Sources* **2016**, *326*, 686–694.
[122] V. Aravindan, D. Mhamane, W. C. Ling, S. Ogale, S. Madhavi, *ChemSusChem* **2013**, *6*, 2240–2244.
[123] B. Li, J. Zheng, H. Zhang, L. Jin, D. Yang, H. Lv, C. Shen, A. Shellikeri, Y. Zheng, R. Gong, J. P. Zheng, C. Zhang, *Adv. Mater.* **2018**, *30*, 1705670.
[124] P. Han, G. Xu, X. Han, J. Zhao, X. Zhou, G. Cui, *Adv. Energy Mater.* **2018**, *8*, 1801243.
[125] J. Boltersdorf, S. A. Delp, J. Yan, B. Cao, J. P. Zheng, T. R. Jow, J. A. Read, *J. Power Sources* **2018**, *373*, 20–30.
[126] L. Que, F. Yu, Z. Wang, D. Gu, *Small* **2018**, *14*, 1704508.
[127] F. Yu, L. Que, C. Xu, L. Deng, Y. Jiang, Y. Xia, Z. Wang, *Chem. Eng. J.* **2020**, *392*, 123795.
[128] F. Wang, C. Wang, Y. Zhao, Z. Liu, Z. Chang, L. Fu, Y. Zhu, Y. Wu, D. Zhao, *Small* **2016**, *12*, 6207–6213.
[129] H. Li, L. Peng, Y. Zhu, X. Zhang, G. Yu, *Nano Lett.* **2016**, *16*, 5938–5943.
[130] D. Yan, J. Zhang, D. Xiong, S. Huang, J. Hu, M. E. Pam, D. Fang, Y. Wang, Y. Shi, H. Y. Yang, *J. Mater. Chem. A* **2020**, *8*, 11529–11537.
[131] Z. Chen, T. Yuan, X. Pu, H. Yang, X. Ai, Y. Xia, Y. Cao, *ACS Appl. Mater. Interfaces* **2018**, *10*, 11689–11698.
[132] M. Park, Y. Lim, J. Kim, Y. Kim, J. Cho, J. Kim, *Adv. Energy Mater.* **2011**, *1*, 1002–1006.
[133] S. S. Zhang, *J. Mater. Chem. A* **2017**, *5*, 14286–14293.
[134] C. Sun, X. Zhang, C. Li, K. Wang, X. Sun, Y. Ma, *Energy Storage Mater.* **2020**, *24*, 160–166.
[135] Y. Guo, X. Li, Z. Wang, H. Guo, J. Wang, *J. Energy Chem.* **2020**, *47*, 38–45.
[136] K. Zou, P. Cai, Y. Tian, J. Li, C. Liu, G. Zou, H. Hou, X. Ji, *Small Methods* **2020**, *4*, 1900763.
[137] X. Zhang, Q. Zhang, X. Wang, C. Wang, Y. Chen, Z. Xie, Z. Zhou, *Angew. Chem. Int. Ed.* **2018**, *57*, 12814–12818.
[138] C. Zhan, K. Zhang, Y. Li, M. Zhang, Z. Shen, *Electrochim. Acta* **2020**, *343*, 136163.
[139] S. Zheng, J. Ma, Z. Wu, F. Zhou, Y. He, F. Kang, H. Cheng, X. Bao, *Energy Environ. Sci.* **2018**, *11*, 2001–2009.
[140] B. D. Boruah, *Energy Storage Mater.* **2019**, *21*, 219–239.

Manuscript received: December 23, 2020
Revised manuscript received: January 28, 2021
Accepted manuscript online: January 29, 2021
Version of record online: February 17, 2021